15- Hardening Soil Model – PLAXIS

This model is the Hardening Soil model as presented in PLAXIS manual. The model is developed using the user-defined material model option in RS[2] and RS[3].

Experimental evidence indicates that the plastic deformation in soils starts from the early stages of loading. To capture such a behavior in a constitutive model the typical elasto-perfect plastic models are not adequate. To simulate such behavior constitutive models that utilize a hardening law after initial yielding are required. The main feature of the Hardening Soil model (Schanz and Vermeer 1999) is its ability to simulate hardening behavior. The hardening in this model is divided to deviatoric and volumetric hardenings by utilizing a shear and a cap yield surface. The model also uses nonlinear elastic behavior that relates the elastic modulus to the stress level.

The model utilizes three yield surfaces that includes deviatoric (shear), volumetric (cap) and tension cut off. The yield surfaces and hardening characteristics of this model are illustrated in Figure 15.1.

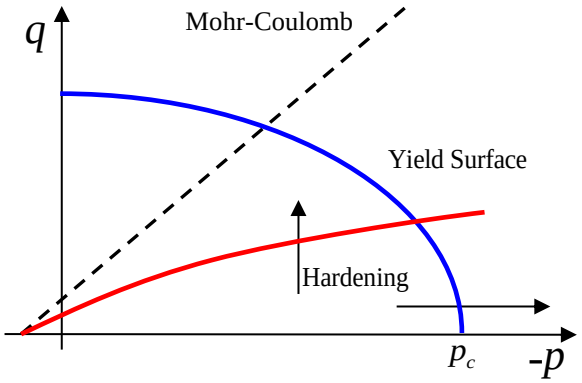

Figure 15.1- The yield surfaces of the Hardening Soil model;
Deviatoric yield surface (red) and elliptical cap (blue)

The formulations of these three mechanisms, definition of yield surfaces and their corresponding plastic potential and hardening law are presented below.

15.1- Deviatoric Hardening Mechanism

The deviatoric mechanism is the core of this model and at it uses the Mohr-Coulomb material properties in its definition and at its ultimate state reaches to the failure defined by corresponding Mohr-Coulomb yield surface. Like Duncan-Chang model this model is formulated to capture that hyperbolic curve that is commonly observed in drained triaxial tests. The yield surface of the deviatoric mechanism is defined as

$$F_s = \frac{q}{E_i(1-q/q_a)} - \frac{q}{E_{ur}} - \varepsilon_q^{p-shear} = 0 \tag{15.1}$$

Where q is the deviatoric stress and $\varepsilon_q^{p-shear}$ is the deviatoric plastic strain generated only by the deviatoric mechanism.

The Mohr-Coulomb function, with ultimate friction angle (φ) and cohesion (c), is used in the definition of q_a.

$$q_a = \frac{q_f}{R_f} \ , \quad q_f = (c\cot\varphi + \sigma_1)\frac{2\sin\varphi}{1-\sin\varphi} \tag{15.2}$$

In above R_f is the failure ratio and one of the material parameters (less than 1.0 with a default value 0.9).

The E_{ur} is the elastic modulus in unloading and reloading

$$E_{ur} = E_{ur}^{ref}\left(\frac{c\cos\varphi+\sigma_1\sin\varphi}{c\cot\varphi+p_{ref}\sin\varphi}\right)^m \tag{15.3}$$

where E_{ur}^{ref} is the reference elastic modulus for unloading/reloading at stress level equal to the reference pressure, p_{ref}. Power m, controls the stress dependency of the elastic modulus and it is within the range of $0.5 < m < 1.0$.

The other parameter in the definition of yield surface, that controls the slope of hyperbolic curve, is E_i

$$E_i = \frac{2E_{50}}{2-R_f} \ , \quad E_{50} = E_{50}^{ref}\left(\frac{c\cos\varphi+\sigma_1\sin\varphi}{c\cot\varphi+p_{ref}\sin\varphi}\right)^m \tag{15.4}$$

In above E_{50}^{ref} is a reference stiffness modulus at the reference pressure.

The hyperbolic curve in a triaxial test that is simulated using Hardening Soil model is illustrated in Figure 15.2. The effects of different material properties are illustrated in this figure.

The hardening in this mechanism is attributed to plastic distortion by direct appearance of the plastic deviatoric strain in the definition of yield function.

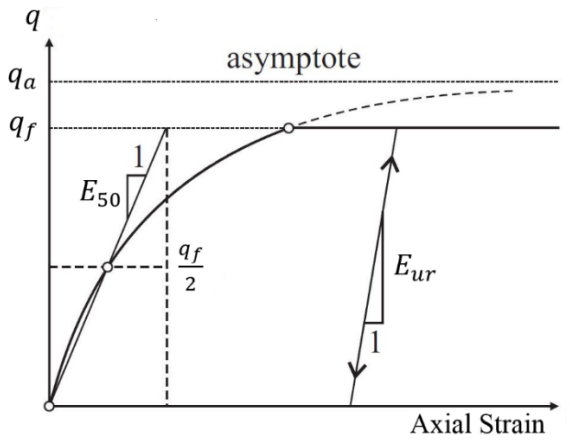

Figure 15.2- Hyperbolic stress-strain curve in a drained compression triaxial test

In RS[2] and RS[3], we introduced a minimum mean effective stress limit (p_{limit}) to prevent stiffness equations (15.3) and (15.4) from returning zero or not a number (NAN). The limit helps ensure the minor principal stress (σ_1) is greater than zero. In general, zero stiffness can cause computational instability which is undesirable. Additionally, yield surface equation (15.1) shows that a zero stiffness in the denominator will cause a computational error. We set p_{limit} to be about 10% of the reference pressure (p_{ref}) as a rule of thumb. However, the user can adjust p_{limit} according to the needs of their simulation.

There are two option for the flow rule for the deviatoric mechanism of this model. The flow rule is defined in terms of the relationship between the plastic volumetric strain and plastic deviatoric strain in a way that

$$\dot{\varepsilon}_v^p = \sin\psi_m \, \dot{\varepsilon}_q^p \tag{15.5}$$

where ψ_m is the mobilized dilation angle.

The first option for calculation of the mobilized dilation angle is based on the stress-dilatancy theory by Rowe (1962). In this theory the mobilized dilation angle is calculated based on the mobilized friction angle φ_m and critical state friction angle φ_{cv} . The essential concept behind the critical state friction angle is that while under shear the material will undergo compression if $\varphi_m > \varphi_{cv}$ and will dilate otherwise.

$$\sin\psi_m = \frac{\sin\varphi_m - \sin\varphi_{cv}}{1 - \sin\varphi_m \sin\varphi_{cv}} \tag{15.6}$$

$$\sin\varphi_m = \frac{\sigma_1 - \sigma_3}{\sigma_1 + \sigma_3 - 2c\cot\varphi} \tag{15.7}$$

$$\sin\varphi_{cv} = \frac{\sin\varphi - \sin\psi}{1 - \sin\varphi\sin\psi} \tag{15.8}$$

In above ψ is the ultimate dilation angle.

The second option for the calculation of dilation angle is a simplification of the former option, and is as flows

$$\text{for } \sin\varphi_m < \frac{3}{4}sin\varphi: \qquad \psi_m = 0 \tag{15.9}$$

$$\text{for } \sin\varphi_m \geq \frac{3}{4}sin\varphi \text{ and } \psi > 0: \qquad \sin\psi_m = \max\left(\frac{\sin\varphi_m - \sin\varphi_{cv}}{1 - \sin\varphi_m \sin\varphi_{cv}}, 0\right)$$

$$\text{for } \sin\varphi_m \geq \frac{3}{4}sin\varphi \text{ and } \psi \leq 0: \qquad \psi_m = \psi$$

$$\text{if } \varphi = 0: \qquad \psi_m = 0$$

The model takes advantage of an optional dilation cut off as well. In case the shearing is extensive and the dilation forces to material to reach to its critical void ratio, at which the plastic flow happens at constant volume, the dilation cut off will stop the volume increase.

$$\text{if } e \geq e_{max}: \qquad \psi_m = 0 \tag{15.9}$$

The relationship between the volumetric strain and void ratio is

$$\left(\varepsilon_v - \varepsilon_v^{initial}\right) = \ln\left(\frac{1+e}{1-e^{initial}}\right) \tag{15.10}$$

where $\varepsilon_v^{initial}$ and $e^{initial}$ are the initial volumetric strain and initial void ratio, respectively.

15.2- Volumetric Hardening Mechanism

The main role of the volumetric mechanism (cap) is to close the elastic domain in space $(p - q)$ on the hydrostatic (p) axis and simulate the densification/compaction of the material.

The cap in the Hardening Soil model is has an elliptical shape with its apex on the q axis:

$$F_c = \left(\frac{q^*}{\alpha}\right)^2 + p^2 - p_c^2 = 0 \tag{15.11}$$

where p_c is the location of the intersection of this yield surface with the p axis, and α is the shape factor for the elliptical shape of the cap. The stress invariant q^* is defined as

$$q^* = \frac{q}{f(\theta)} \ , f(\theta) = \frac{3-\sin(\varphi)}{2\left(\sqrt{3}\cos(\theta)-\sin(\theta)\sin(\varphi)\right)} \tag{15.12}$$

The hardening for these yield surfaces is considered for p_c and it is attributed to volumetric plastic strain generated only by the cap yield surface.

$$\varepsilon_v^{p-cap} = \frac{\beta}{1-m}\left(\frac{p_c}{p_{ref}}\right)^{1-m} \quad or \quad \dot{p}_c = \frac{p_{ref}}{\beta}\left(\frac{p_c}{p_{ref}}\right)^m \tag{15.13}$$

where β is another parameter for this model that controls the hardening of the cap.

The cap parameters α and β are not direct parameters of the model. They are evaluated from the combination of other parameters especially E_{oed} and K_0^{nc}. These last two parameters are material parameters for the Hardening Soil model and can be evaluated from an oedometer test. K_0^{nc} is the coefficient of lateral pressure for normal consolidation, and E_{oed} in an odometer test is the slope of the variation of axial stress versus axial strain. E_{oed}^{ref} is the slope of the aforementioned curve at axial stress equal to the reference pressure.

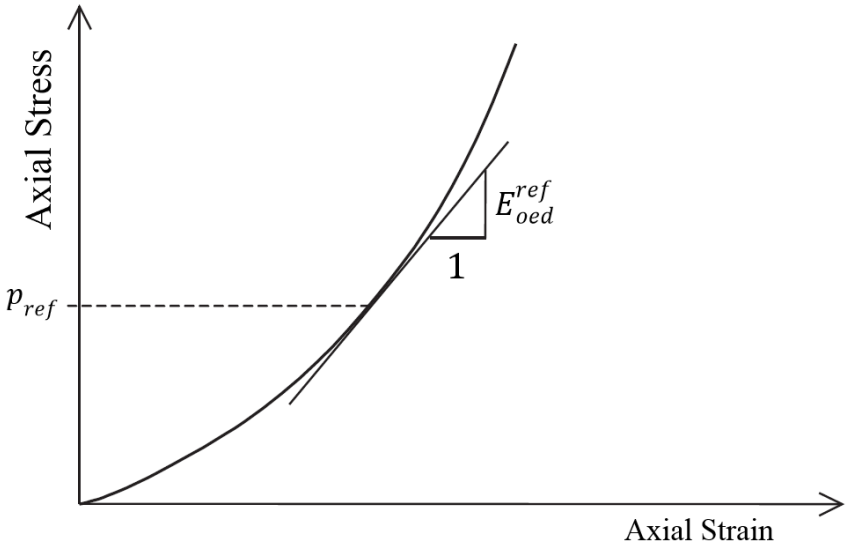

Figure 15.3- Variation of axial stress versus axial strain in an oedometer, and definition of E_{oed}^{ref}

The cap parameters α and β should be evaluated in a way that when simulating an odometer test, the test results generate E_{oed} and K_0^{nc} . The assumptions for the evaluation of the cap parameters by simulating an oedometer test are that

- the state of stress is at K_0^{nc} condition with the axial stress equal to the reference pressure
- a strain controlled oedometer test is simulated by an increment of axial strain
- in this loading process both the deviatoric and volumetric mechanisms are active
- the parameters α and β should be found in a way that $K_0^{nc}$and E_{oed}^{ref} are generated by the updated state of stress

15.3- Tension Cut off

This mechanism is to incorporate the tensile strength of the material to this model. In this mechanism the minor principal stress is limited to the tensile strength of the material. The flow rule is associated and the mechanism has no hardening.

$$F_T = \sigma_1 - T = 0 \tag{15.14}$$

In above T is the tensile strength of the material.

15.4- Examples

Figure 15.4 and 15.5 shows the numerical results of drained triaxial tests on Berlin sand-III. A comparison is made between the results obtained by Hardening Soil model in PLAXIS and simulation results of the Hardening Soil model in Rocscience products. The model parameters are presented in Table 15.1.

Characteristics	Values for Berlin Sand III
p_{ref} (kPa)	100
E_{50}^{ref} (MPa)	105
E_{ur}^{ref} (Ma)	315
E_{oed}^{ref} (MPa)	105
m	0.55
ν (Poisson's ratio)	0.2
K_0^{nc}	0.38
φ (degrees)	38
ψ (degrees)	6

c (kPa)	1.0
Failure ratio	0.9
Tensile strength (kPa)	0

Table 15.1. Hardening Soil model parameters for Berlin sand-III (PLAXIS 2014)

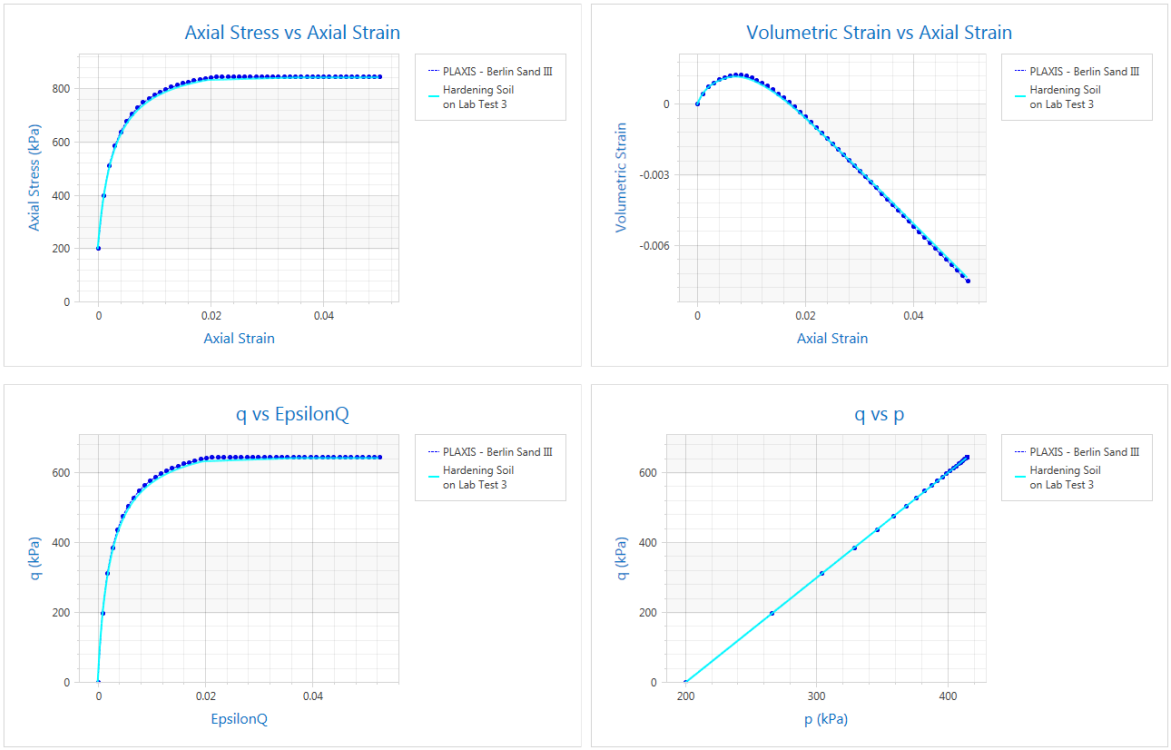

Figure 15.4. Stress paths of drained triaxial tests on Berlin sand-III

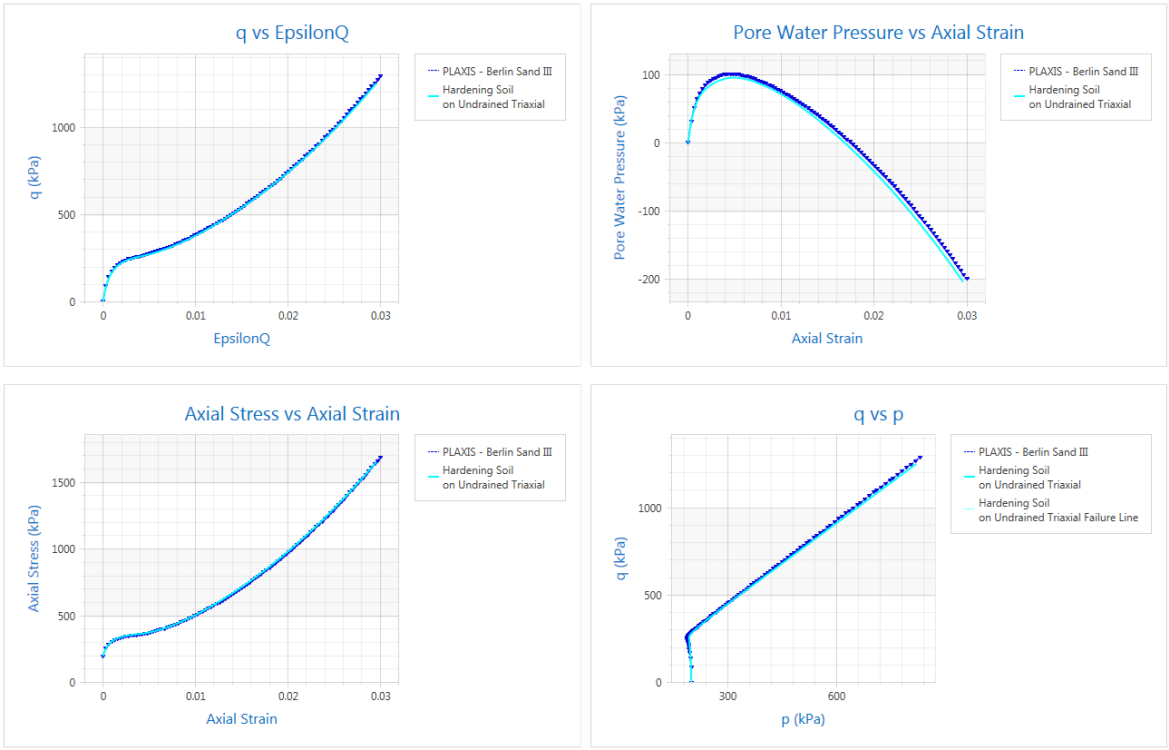

Figure 15.5. Stress paths of undrained triaxial tests on Berlin sand-III

References

Schanz, T., P. A. Vermeer, and P. G. Bonnier. "The hardening soil model: formulation and verification." Beyond 2000 in computational geotechnics (1999): 281-296.

Plaxis, "User's manual of PLAXIS." (2014).